

## Comparative adsorption study for the removal of Alizarin Red S and patent Blue VF by using mentha waste

RAIS AHMAD\* and RAJEEV KUMAR

Environmental Research Laboratory, Department of Applied Chemistry,  
Faculty of Engineering and technology, Aligarh Muslim University, Aligarh - 202 002 (India)

(Received: May 10, 2008; Accepted: June 14, 2008)

### ABSTRACT

The adsorption of the Alizarin Red S (ARS) and Patent Blue VF (PBVF) from aqueous solution onto agricultural waste mentha has been investigated. The effects of initial dye concentration, contact time, pH, temperature and ionic strength were studied in a batch system. ARS and PBVF adsorption onto mentha increased to minor extent with decreasing pH. Adsorption capacities of dyes increased with contact time, initial concentration, and temperature for both ARS and PBVF. Adsorption of ARS on mentha is more favorable than PBVF. The adsorption of ARS and PBVF was spontaneous and endothermic as concluded from thermodynamic assays.

**Key words:** Adsorption, Mentha waste, Kinetics, Thermodynamics, Isotherms.

### INTRODUCTION

Dyes are common constituents of effluents discharged by various industries, particularly the textile industry. The presence of very small amounts of dyes in water is highly visible and undesirable<sup>1-2</sup>. Dyes may significantly affect photosynthetic activity of aquatic life due to reduced light penetration and may also be toxic to some aquatic life due to the presence of aromatics, metals, chlorides, etc. in them<sup>3-6</sup>. Total dyes consumption of the textile industry worldwide is more than 10 000 tones /year, with an estimated 90% in fabrics industries. It is reported that approximately 100 tones of dyes are discharged into waste streams by the textile industry per year<sup>7</sup>. Alizarin Red S and Patent Blue VF are the most hazardous dyes, responsible for several hazardous effects like skin and eyes irritation when comes in contact and possible cancer hazard.

Although conventional chemical and

biological treatments have been applied for the removal of dyes from textile wastewater. These processes are insufficient in removing dye contaminants since dyes are stable to light, heat, and oxidizing agents<sup>8-11</sup>. Adsorption has evolved as one of the most effective physical processes for purification of the textile wastewaters since it can produce high-quality water and also be a process that is economically feasible<sup>12</sup>. The most commonly used adsorbent for colour removal is activated carbon<sup>13</sup>. However, due to the problem of activated carbon's cost, the use of alternative adsorbents is attractive. Several researchers have been studying the use of other materials, such as industrial waste, agricultural by products, minerals eg., bottom ash<sup>14</sup>, peat<sup>15</sup>, montmorillonite<sup>16</sup>, orange peel<sup>17</sup> etc.

In this study we investigated the mentha waste as a potential biosorbent. India is the leading producer of mentha in the world. China and Brazil follow India in the list of major producers on 2nd

and 3rd place. The oil is extracted by steam distillation from the fresh or partly dried plant and the yield is 0.1-1.0%. Around 96-99% de-oiled mentha plant is dumped as agricultural waste.

The objective of this study was to explore the potential use of agricultural waste mentha to remove Alizarin Red S and Patent Blue VF dyes from an aqueous solution in batch.

## MATERIAL AND METHODS

### Adsorbate

The dyes, Alizarin Red S, molecular formula ( $C_{14}H_7NaO_7S$ ), molecular weight (342.26), C.I. (58005), ( $\lambda_{max}$  425) and Patent Blue VF molecular formula ( $C_{27}H_{31}N_2NaO_6S_2$ ) ( $\lambda_{max}$  635 nm), molecular weight (566.66), C.I. (42045) was obtained from CDH New Delhi, India. The stock solution was prepared by dissolving accurately weighted dye in double distilled water. The structure of ARS and PBVF is shown in Fig. 1.

### Preparation and characterization of adsorbent

Mentha was collected from local mentha oil distillation plant. The dry leaves were removed and the collected biosorbent was extensively washed with hot water and dried. Afterwards, the mentha was crushed. The resulting material sieved by the 100BSS mesh and subsequently washed with double distilled hot water for several time, and then dried in oven at 60°C for 24 h. Mentha surface was characterized by scanning electron microscopy. SEM images clearly show the irregular and porous surface of mentha particles. SEM images of mentha before and after adsorption are shown in Fig. 2.

### Adsorption studies

The adsorption capacity of mentha for ARS and PBVF were studied in batch process. 0.5g of mentha was placed in a 250 ml standard flask containing 50 ml of dye solution (concentration range 20 -100 mg /L) at contact time ranging from 5-180 min. The dye remained in the solution was determined by double beam UV-vis spectrophotometer (Elico SL 164 model) with 1.0 cm path length cell. Absorbance measurements were made at the maximum wavelength of ARS at 425 and 638 nm for PBVF. The amount of dye uptake by the biosorbent was calculated by applying the

equation:

$$q = (C_0 - C_e)V / M \quad \dots(1)$$

Where  $C_0$  and  $C_e$  (mg/L) are the liquid-phase concentrations of dye at initial and equilibrium, respectively.  $V$  is the volume of the solution (l) and  $W$  is the mass of dry adsorbent used (g).

## RESULTS AND DISCUSSION

### Effect of contact time

The effects of contact time in the range 5–180 min were studied in the concentration range 20-50 mg/L of dyes solution at 30°C. The uptake of the ARS and PBVF as a function of contact time is shown in the Fig. 3 & 4. The uptake of dyes increased with increased contact time. Maximum quantitative removal of dyes from an aqueous solution was obtained less than 120 min. However, the experimental data were measured at 180 min to make sure that full equilibrium was attained. Beyond 120 min, there was no increase in dyes removal.

### Effect of pH

The effect of solution pH on the adsorption of ARS and PBVF is shown in Fig 5. For both the dyes, the amount of adsorption decreases when the pH increased. Low pH was found to be favorable for maximum adsorption of dyes. At lower pH, the positive charge density on the surface of mentha increased which favors the adsorption of negatively charge dyes through the electrostatics force of attraction<sup>18</sup>.

### Effect of concentration

The effect of the amount of adsorbate on the rate of uptake of dyes was studied at various concentrations. The results are shown in Fig. 6. It is obvious that by increasing the initial dyes concentration, the uptake of the dyes increase with increasing the concentration of dyes. It might be explained by the fact that in dilute solution the numbers of dye molecules are less than concentrated.

### Effect of salt

The effect of salt on the adsorption capacity was carried out by varying the concentration of salt in the range 10-100 mg/L. Results indicate the

slightly increase in the adsorption of ARS while in case of PBVF, no change in adsorption as shown in Fig. 7. The presence of external electrolyte rise the adsorption of ARS, it means that an electrostatic interaction occurs between ARS and mentha surface.

### Effect of temperature

Effect of temperature on adsorption capacity was studied at the temperature 30, 40 and 50°C. The results are shown in Fig. 8 and 9. There was gradual increase in the adsorption capacity of mentha as the temperature increase 30-50°C and

shows that endothermic nature of adsorption. The enhancement in adsorption with temperature may be due to increase in the number of active surface sites available for adsorption on adsorbent, increase in the porosity and in the total pore volume of the adsorbent. This may also be as a result of an increase in the mobility of the dye molecule with increase in their kinetic energy and the enhanced rate of intra-particle diffusion of adsorbate with the rise in temperature<sup>19</sup>.

### Adsorption isotherm

The equilibrium adsorption data were

**Table 1: Langmuir and Freundlich constant for the adsorption of Alizarin Red S and Patent Blue VF at 30 °C**

Dye	Langmuir isotherm		Freundlich isotherm			
	$b \times 10^{-4}$	Q0	R2	Kf	1/n	R2
ARS	7.085	94.59	0.991	0.065	0.996	0.998
PBVF	3.839	16611	0.993	0.078	0.907	0.997

**Table 2: Thermodynamic parameters for ARS adsorption**

Temperature (K)	Kc	$\Delta G^0$	$\Delta H^0$	$\Delta S^0$	R <sup>2</sup>
303	1.078	-2.714			
313	1.203	-3.124	43.557	0.163	.9135
323	1.56	-4.187			

**Table 3: Thermodynamic parameters for PBVF adsorption**

Temperature (K)	Kc	$\Delta G^0$	$\Delta H^0$	$\Delta S^0$	R <sup>2</sup>
303	0.672	-1.629			
313	0.967	-2.515	45.483	0.163	.9938
323	1.17	-3.140			

**Table 4: Values of kinetic parameters for ARS and PBVF at the concentration of 50 mg/l**

Dye	Pseudo first order kinetics			Pseudo second order kinetics		
	qe(cal)(mg/g)	$k_1(\text{min}^{-1})$	R <sup>2</sup>	qe(cal) (mg/g)	$k_2(\text{g/mg min})$	R <sup>2</sup>
ARS	1.192	0.375	0.952	2.188	0.035	0.995
PBVF	1.421	0.246	0.990	6.13	0.020	0.949

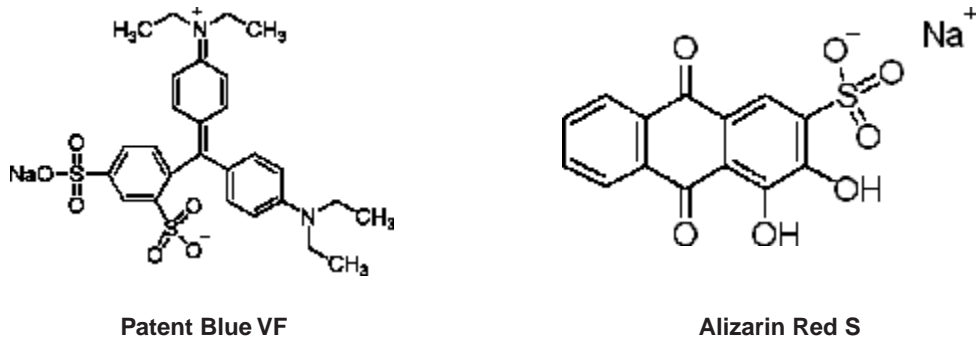
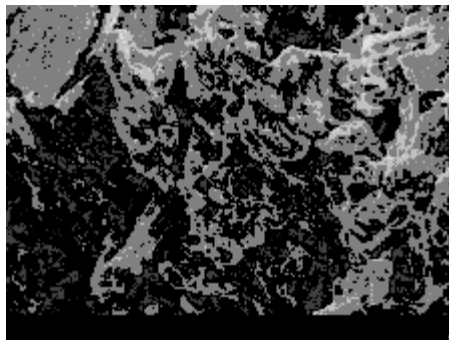
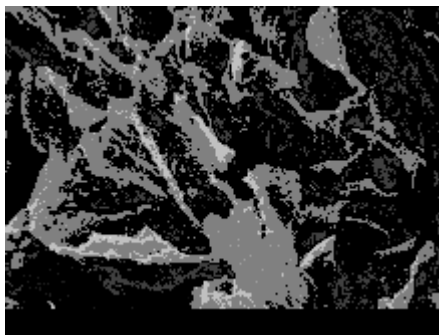


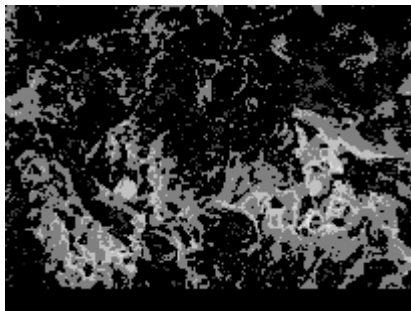
Fig. 1: Structure of dyes



(a) Before Dye adsorption



(b) After ARS adsorption



(c) After PBVF adsorption

Fig. 2: SEM images of mentha before and after adsorption

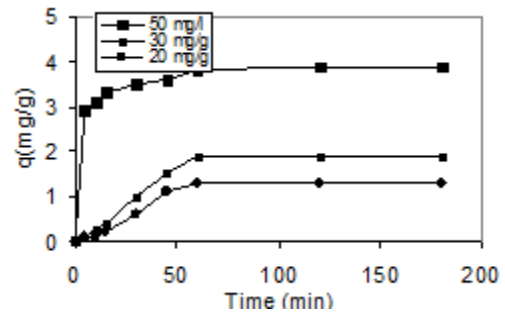


Fig. 3: Effect of contact time for the uptake of ARS

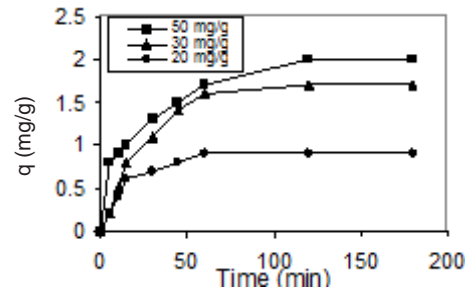


Fig. 4: Effect of contact time for the PBVF

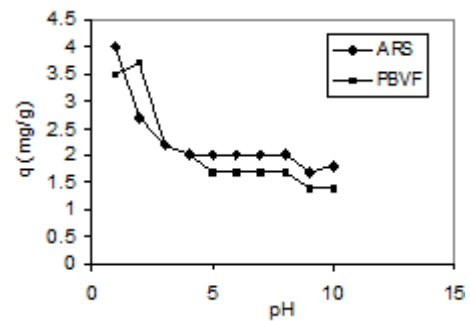


Fig. 5: Effect of pH

analyzed using the well known Langmuir and Freundlich models. Langmuir model is based on the assumption of homogeneity, such as equally available adsorption sites, monolayer surface coverage and no interaction between adsorption species while Freundlich adsorption isotherm is based on the assumption that the sites on the surface of adsorbent have different binding energies. The linear form of the Langmuir and Freundlich isotherm models are given by following equations, respectively:

$$1/x/m = 1/Q_0 b c + 1/Q_0 \quad \dots(2)$$

$$\dots(3)$$

Where  $x/m$  is dye uptake in mg/g,  $c$  is equilibrium concentration of dye (mg/l),  $Q_0$  and  $b$  are the Langmuir constant related to the adsorption

capacity and adsorption energy.  $K_f$  is the Freundlich constant and  $n$  the Freundlich exponent. The plots of Langmuir and Freundlich adsorption isotherm models for ARS and PBVF are shown in Fig. 10 and 11 at 30 °C. Langmuir and Freundlich parameters were calculated from the slope and intercept of their respective plots ( $1/x/m$  Vs  $1/c$  and  $\ln 1/x/m$  Vs  $\ln c$ ) and the values are listed in the Table 1.

### Adsorption thermodynamics

Thermodynamic parameters such as change in free energy ( $\Delta G^0$ ), enthalpy ( $\Delta H^0$ ), and entropy ( $\Delta S^0$ ) were determined using the following eqn.

$$\dots(4)$$

Where  $T$  is temperature in kelvin and  $R$  is gas constant.  $\Delta H^0$ , and  $\Delta S^0$  were calculated from following eq.

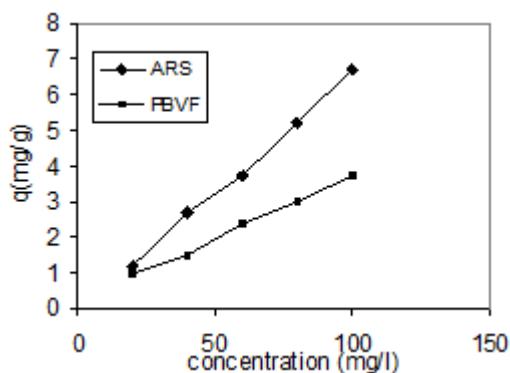


Fig. 6: Effect of concentration

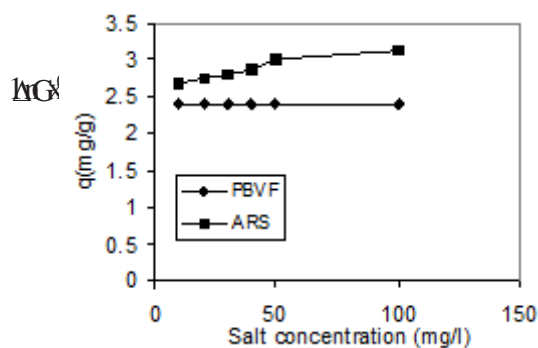


Fig. 7: Effect of salt

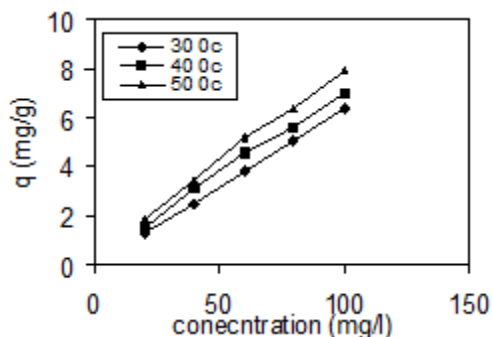


Fig. 8: Effect of temperature for the ARS adsorption

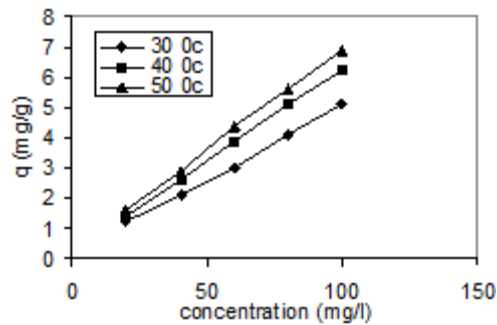


Fig. 9: Effect of temperature for the PBVF adsorption

$$\ln Kc = \Delta S^0 / R - \Delta H^0 / RT \quad \dots(5)$$

The values of  $(\Delta H^0)$ , and  $(\Delta S^0)$  were calculated from the slope and intercept of plots between  $\ln Kc$  versus  $1/T$ . The calculated values of  $(\Delta G^0)$ ,  $(\Delta H^0)$ , and  $(\Delta S^0)$  are listed in Table (2 & 3). The positive value of enthalpy indicated the

endothermic nature of the adsorption interaction and negative values of  $\Delta G^0$  shows the feasibility of adsorption of ARS and PBVF onto mentha waste.

**Adsorption kinetics**

Feasibility and efficiency of adsorption process can be determined by the kinetic study. Kinetics data of ARS and PBVF was evaluated by

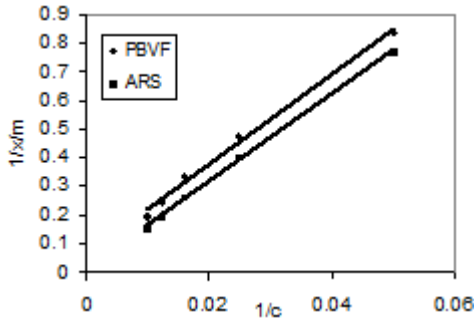


**Fig. 10: Langmuir adsorption isotherm for ARS and PBVF at 30°C**

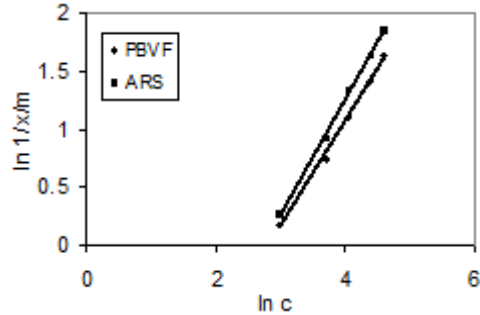


**Fig. 11: Freundlich adsorption isotherm for ARS and PBVF at 30°C**

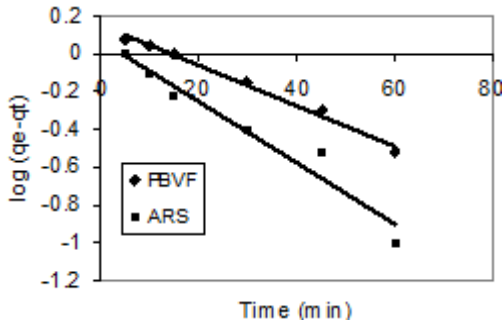


**Fig. 12: Pseudo first order kinetics for the ARS and PBVF adsorption at the concentration 50mg/g**

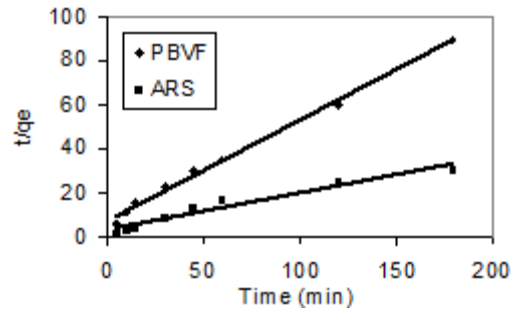


**Fig. 12: Pseudo second order kinetics for the ARS and PBVF adsorption at the concentration 50mg/l**

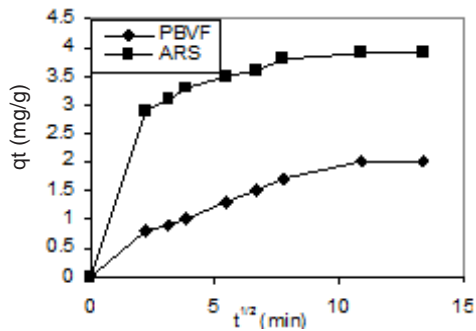


**Fig. 14: Intra - particle diffusion mechanism for ARS and PBVF adsorption at the concentration 50ml/l**

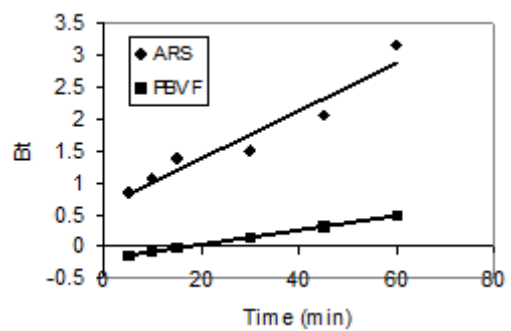


**Fig. 15: Bt Vs Time (min)**

the pseudo first and pseudo second order kinetic models. Pseudo first order<sup>20</sup> (eq. 6) and pseudo second order<sup>21</sup> (eq. 7) equations are shown as:

$$\log (q_e - q_t) = \log q_e - k_1 t/2.303 \quad \dots(6)$$

$$\dots(7)$$

Where  $q_e$  and  $q_t$  are the amount adsorbed at equilibrium and time  $t$ , respectively. Where  $k_1$  and  $k_2$  are pseudo first and pseudo second order rate constant. Fig. 12 and 13 shows linear plots of pseudo first and pseudo second order kinetic models for ARS and PBVF adsorption. The values of all the parameters are given in Table 4. The result shows good agreement of experimental data with pseudo second order model. As can be seen from Table 4,

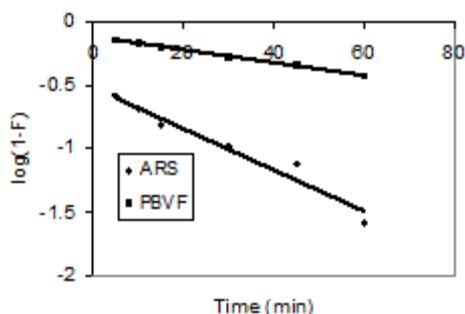


Fig. 16:  $\log (1-F)$  vs Time (min)

the calculated value of  $q_e$  has close agreement with the experimental data and good correlation coefficient for pseudo second order. It can be said that both dyes adsorption system followed pseudo second order kinetic model.

**Sorption mechanism**

The intra-particle diffusion parameter,  $k_i$  ( $\text{mg/g min}^{0.5}$ ) is defined by the following eq.

$$\dots(8)$$

Where  $q_t$  is the amount of dyes adsorbed ( $\text{mg/g}$ ) at time  $t$ ,  $k_i$  is intra-particle diffusion constant ( $\text{mg/g min}^{0.5}$ ), and  $c$  is the intercept. The plots of  $q_t$  Vs  $t^{0.5}$  are linear (Fig. 14). If the value of  $c$  is zero, then the rate of adsorption is controlled by intra-particle diffusion for the entire adsorption period,

but the values of the  $c$  are not zero so the adsorption process was controlled by film diffusion for ARS and PBVF. ARS has the  $k_i = 0.268 \text{ mg/g min}^{0.5}$  and  $c = 1.88$  while PBVF has the  $k_i$  value 0.143 with  $c = 0.391$  at the concentration 50  $\text{mg/L}$ .

The film-diffusion model of Boyd is expressed as:

$$\dots(9)$$

$$\dots(10)$$

Where  $F$  is the fractional attainment of equilibrium, at different times,  $t$ , and  $Bt$  is a function of  $F$  (vice versa)

$$\dots(11)$$

Where  $q_t$  and  $q_e$  are the dye uptake ( $\text{mg/g}$ ) at time  $t$  and at equilibrium, respectively. The Boyd plots of ARS and PBVF shown in Fig. 15. The plot  $Bt$  Vs Time shows linearity with straight lines without passing through the origin in case of both dyes adsorption. This suggests film diffusion as rate determining process<sup>22</sup>

To reconfirm the above observations Mckay's plots  $\log (1-F)$  Vs Time (Fig. 16) were plotted at 50  $\text{mg/l}$  concentration of both dyes and straight lines deviating from origin were obtained. These observations support the rate of adsorption of ARS and PBVF over mentha waste undergo via internal transport mechanism<sup>23</sup>.

**CONCLUSIONS**

Mentha waste is a locally available and low-cost material that can be used as an alternative adsorbent for removal the acidic dyes Alizarin Red S and Patent Blue VF from aqueous solutions, without any laborious pre-treatment. The adsorption of ARS and PBVF depended on initial dye concentration, temperature and pH. Quantitative adsorption of ARS and PBVF were obtained within a very short time. The equilibrium was stabilized less than 120 min. In the presence of external electrolyte, there is electrostatic interaction between ARS and mentha. Adsorption obeys both Freundlich and Langmuir isotherms. The positive value of " $H^0$ " indicates the endothermic nature of dyes adsorption.

## REFERENCES

1. Crini G., *Bioresour. Technol.*, **97**: 1061 (2006).
2. Robinson, T., McMullan G., Marchant R. and Nigam P., *Bioresour. Technol.*, **77**: 247 (2001).
3. Banat I.M., Nigam P., Singh D. and Marchant R., *Bioresour. Technol.*, **58**: 217 (1996).
4. Mishra G. and Tripathy M., *Colourage*, **40**, 35 (1993).
5. Fu Y. and Viraraghavan T., *Bioresour. Technol.*, **79**: 251 (2001).
6. Zollinger H., Azo dyes and pigments, *Colour Chemistry-Synthesis, Properties and Applications of Organic Dyes and Pigments*, VCH, New York 92-100 (1987).
7. Wong Y.C., Szeto Y.S., Cheung W.H., McKay G., *Langmuir*, **19**: 7888 (2003).
8. Jyun T. K., Chulhwan P., Eung B. S., Sangyong K., *Desalination*, **49**: 161 (2004).
9. Jyun T. K., Chulhwan P., Jeongmook Y., Sangyong K., *J. Hazard. Mater.*, **B112**: 95 (2004).
10. Bell J., Buckley C. A., *Water SA*, **29**, 129 (2003).
11. Herrera F., Lopez A., Mascolo G., Albers P., Kiwi J., *Water Res.*, **35**: 750 (2001).
12. Ozcan A., Ozcan A. S., *J. Hazard. Mater.*, **B125**: 252 (2005).
13. Oliveira L. C. A., Rios R. V. R. A., Fabris J. D., Garg V., Sapag K., Lago R. M., *Carbon*, **40**: 2177 (2002).
14. Gupta V.K., Mittal A., Krishnan L. and Gajbe V., *Sep. Purif. Technol.*, **40**: 87 (2004).
15. Ho, Y. S., McKay G., *Chem. Eng. J.*, **70**: 115 (1998).
16. Yermiyahu, Z., Lapidés I. and Yariv S., *Clay Miner.*, **38**: 483 (2003).
17. Namasivayam C., Muniasamy N., Gayatri K., Rani M. and Ranganathan K., *Bioresour. Technol.* **57**: 37 (1996).
18. Muhammad J.Iqbal, Muhammad N Ashiq., *J. Hazard. Mater.*, **B139**: 57 (2007).
19. Zu mriye Aksu, Ayeslydil Tatly, Ozlem Tunc, *Chemical Engineering Journal* doi:10.1016/j.ccej.2007.11.005 (2007).
20. Periasamy K., Namasivayam C., *Ind. Eng. Chem. Res.*, **33**: 317 (1994).
21. Ho Y.S., McKay G., *Process Biochem.*, **38**: 1047 (2003).
22. Hameed B.H., El-khariary M.I., *J.Hazard. Mater.* (2007),doi:10.1016/j.jhazmat.2007.10.017.
23. Alok Mittal, *J. Hazard. Mater.*, **B128** 233 (2006).